Chemistry & Biology, Vol. 10, 25–34, January, 2003, ©2003 Elsevier Science Ltd. All rights reserved. DOI 10.1016/S1074-5521(02)00296-X

An Unusual Phylogenetic Variation in the Metal Ion Binding Sites of Porphobilinogen Synthase

Eileen K. Jaffe*
Institute for Cancer Research
Fox Chase Cancer Center
7701 Burholme Avenue
Philadelphia, Pennsylvania 19111

Summary

Porphobilinogen synthase (PBGS), which catalyzes the first common step in tetrapyrrole biosynthesis, contains a unique phylogenetic variation in the use of metal ions. Using sequence, structure, and enzymological information, this work codifies the phylogenetic segregation of metal utilization in PBGS from archaea, bacteria, and eucarya. All PBGS contain an active site metal binding sequence, determined herein to be either DXCXCX(Y/F)X_3G(H/Q)CG or DXALDX(Y/F)X_3G(H/Q)DG. The former dictates a requirement for zinc. Most PBGS that do not require zinc require magnesium and/or potassium instead. Most PBGS are also found to contain the binding determinants for an allosteric magnesium that resides outside the active site. The phylogenetic distribution of PBGS metal ion utilization suggests that the primordial PBGS required zinc and supports a hypothesis that the loss of the zinc site was concurrent with the advent of oxygenic photosynthesis.

Introduction

Throughout evolution the tetrapyrrole pigments have been critical participants in metabolism. For example, cofactor F_{430} functions in methanogenesis, the chlorophylls function in photosynthesis, and hemes function in a plethora of essential processes including aerobic electron transport and detoxification. The first common step in tetrapyrrole biosynthesis is the asymmetric condensation of 5-aminolevulinic acid to form the monopyrrole porphobilinogen [1]. Four molecules of porphobilinogen form each tetrapyrrole. Once the common cyclic tetrapyrrole core is formed, the pathway diverges to create the individual cofactors. These specialized pathways involve insertion of specific metal ions such as Fe (in heme), Ni (in F_{430}), Co (in B_{12}), and Mg (in chlorophyll) into the center of the tetrapyrrole, as well as additional chemical modifications. This report concerns a unique phylogenic variation in metal ion utilization in the first common enzyme, porphobilinogen synthase (PBGS), also known as δ-aminolevulinic acid dehydratase.

The metal ions of PBGS can be divided into those that reside at the enzyme active site and those that reside at an allosteric site, both of which are present in many PBGS. The active site metal ions vary between zinc and magnesium and/or potassium. The PBGS family of enzymes is unique among known enzymes in having a variable use of zinc and magnesium or potassium at the active site. Zinc is a soft transition element without significant discrimination for first coordination sphere ligands or ligation geometry [2]. The ubiquitous nature of zinc and its flexible coordination chemistry contributes to the wide use of zinc at enzyme active sites. Magnesium on the other hand is an alkaline earth element with a significant preference for oxygen ligands in a rigid octahedral geometry [2]. However, both zinc and magnesium ions are found only in the +2 ionization state. Since a monovalent cation, potassium, can replace the magnesium in some PBGS, charge alone is not the sole determinant of function. Furthermore, monovalent cations generally have a larger number of ligands than do zinc or magnesium, indicating further maleability. The variation in the allosteric metal binding site of PBGS is less complex. Those PBGS that contain the allosteric site bind magnesium at this site, whereas other PBGS simply do not have this metal ion binding site. The current work defines the sequence determinants for the active site metal ions and the allosteric magnesium of the PBGS family of enzymes. Because magnesium can act at both the active site and the allosteric site, care is taken to thwart confusion. Historically, the allosteric magnesium has also been called MgC.

Introductions to biochemical manuscripts on PBGS often contain generalizations about variations in metal ion usage and stoichiometry. As the data on purified proteins has increased along with sequence data and crystal structures, it became clear that these generalizations (e.g., "some PBGS use zinc and some use magnesium") were misleadingly simplistic and often were simply incorrect. The current work is intended in part to provide a suitable reference for the variation in metal ion utilization by the PBGS family of enzymes.

Current databases contain PBGS sequences from ~130 different species that each consist of a highly conserved ~330 amino acid core. PBGS X-ray crystal structures are available from four species, which are yeast (e.g., [3, 4]), *E. coli* (e.g., [5]), *P. aeruginosa* [6, 7], and human (N.L. Mills-Davies, submitted), each with various active site ligands, and all show a common homo-octameric structure. Each PBGS subunit contains an αβ barrel that houses the active site as well as an N-terminal arm that is involved in extensive intersubunit interactions. The crystal structures are essential to defining the sequence determinants that dictate metal ion binding.

The structure of *E. coli* PBGS (PDB code 1L6S) is illustrated in Figure 1 and serves to illustrate the common metal binding variations in PBGS structures. Each *E. coli* PBGS monomer contains two metal ions, neither of which is phylogenetically conserved. The active site contains a zinc ion that is essential to *E. coli* PBGS activity but whose three cysteine ligands are not present in many PBGS. This zinc functions in the binding and reactivity of the second substrate molecule [8]. Details of the zinc site are illustrated in Figure 1B. In addition, there is an allosteric magnesium that is seen bound at

*Correspondence: ek_jaffe@fccc.edu

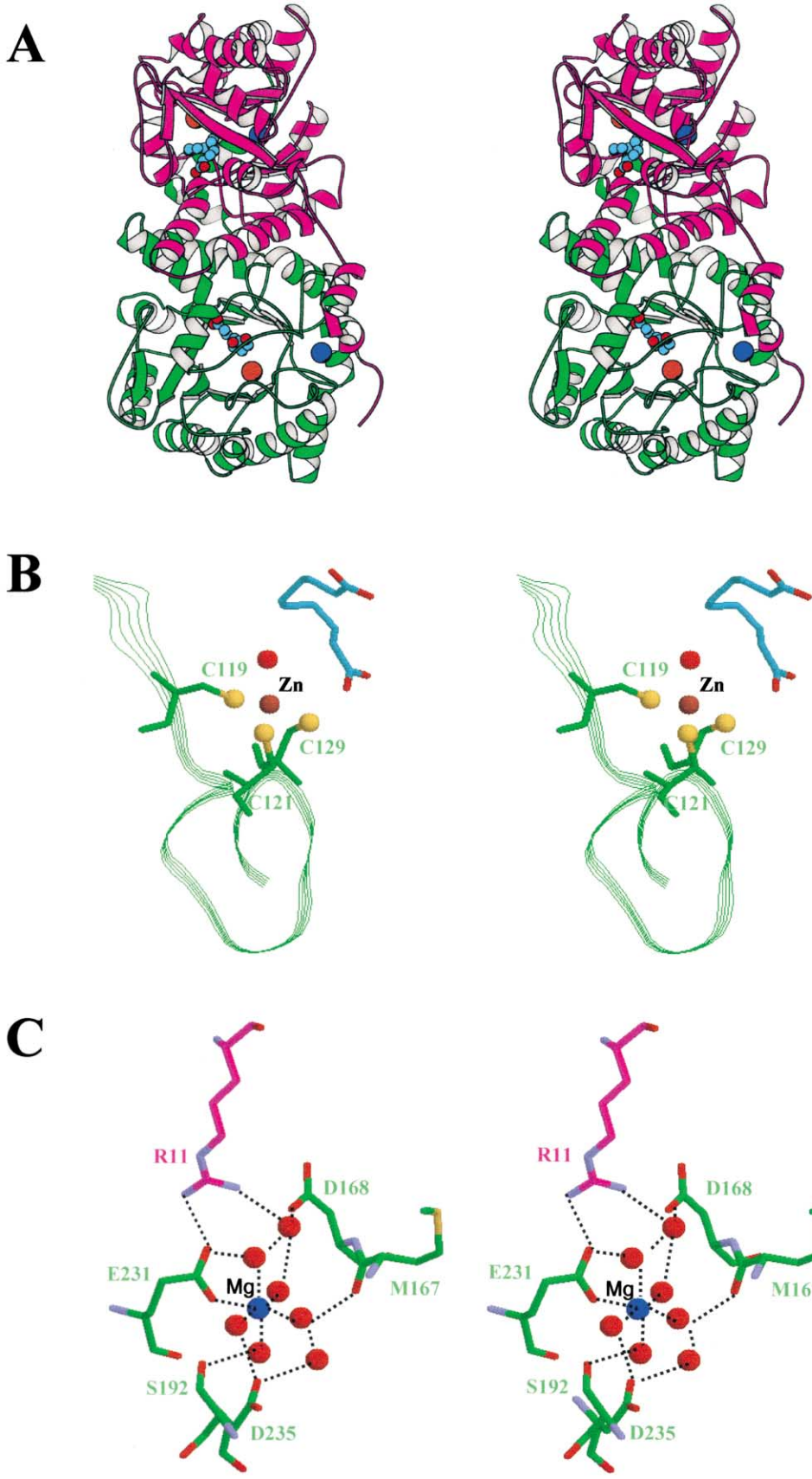
A
B
C119
Zn
C129
C121
C119
Zn
C129
C121
C
R11
D168
E231
Mg
M167
S192
D235
R11
D168
E231
Mg
M167
S192
D235

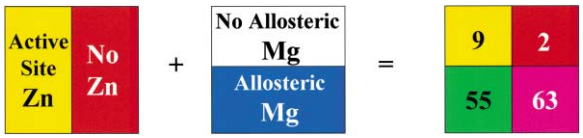

Figure 2. A Proposal for a Novel Classification of PBGS According to the Independently Segregating Criteria of Whether or Not There Is an Active Site Zinc and Whether or Not There Is an Allosteric Magnesium

On the left side of the equation yellow corresponds to the cysteine-rich active site sequence DXCXCX(Y/F)X_3G(H/Q)CG where the underlined cysteines are seen bound to zinc in Figure 1B. Red corresponds to the alternate aspartate-rich active site sequence DXALDX(Y/F)X_3G(H/Q)DG that does not bind zinc. Blue and white respectively correspond to the independently segregating sequence that corresponds to the presence (R$X_{\sim 164}$D$X_{\sim 65}$EXXXD) or absence (X$X_{\sim 164}$D$X_{\sim 65}$XXXRD) of the allosteric magnesium. The underlined residues are the significant variables. On the right side of the equation the color in each quadrant is an admixture of the components (e.g., PBGS that use both an active site zinc [yellow] and an allosteric magnesium [blue] are illustrated as green [yellow + blue]). The numbers inside the quadrants quantify the number of species in the sequence databases that are found to have a PBGS with the corresponding metal binding determinants.

the interface of each $\alpha\beta$ barrel with the N-terminal arm of a neighboring subunit; structural details are in Figure 1C. The sequence determinants for binding the allosteric magnesium are not present in all PBGS.

Figure 2 illustrates a novel schematic for classifying the PBGS into four groups on the basis of whether or not they use an active site zinc and whether or not they use an allosteric magnesium. The two metal binding sites are found to segregate independently. Approximately one-half of the currently available sequences encode an active site zinc requirement and one-half do not. The active site zinc has been correlated with sensitivity of these PBGS to inhibition by the environmental toxin lead [9, 10]. In contrast to the active site metal pattern distribution, more than 90% of the PBGS sequences contain the determinants for allosteric magnesium binding. The presence of the allosteric magnesium confounds unequivocal experimental determination of the role of an active site magnesium. The current analysis traces the phylogenetic segregation of these metal binding traits of PBGS and comments on the evolutionary forces that might have driven the unique variation of active site metal ions in the PBGS proteins.

Results and Discussion

The Metal Ion Binding Sequences of PBGS

Here are described the sequences that determine the individual presence or absence of the two different metal ions shown in Figure 1. The active site metal binding sequence is considered first, and the allosteric magnesium binding sequence is considered second.

The Active Site Metal Binding Sequences

For the following discussion, the PBGS active site residues are considered as amino acids within 8 Å of enzyme-bound porphobilinogen in the human PBGS crystal structure (PDB code 1E51). These 52 residues are phylogenetically invariant or highly conserved, with the exception of the active site metal specificity determinants. An alignment of active site residues for the PBGS sequences culled from GenBank and other web-searchable genomes is presented as Figure 3. The analysis makes use of the NCBI taxonomy resource, www.ncbi.nlm.nih.gov/Taxonomy/taxonomyhome.html, and incorporates experimental data from those PBGS that have been purified and characterized in terms of their metal ion-dependent kinetic properties [11–18]. As illustrated in Figure 2, PBGS family members can be functionally described in terms of those that require zinc and those that do not, a property that is related to the sequence composition of the active site metal binding region [19]. Generally, we find that this metal binding sequence segregates by taxonomic family.

For zinc-requiring forms, the catalytic zinc ion of PBGS is bound to a short cluster of three cysteine residues [3], which is an unusual ligation scheme for a catalytic zinc and is illustrated in Figure 1B. The current analysis of the PBGS sequences reveals the general sequence of the zinc binding motif as DXCXCX(Y/F)X_3G(H/Q)CG wherein X has a limited variability (see Figure 3). Initial identification of this sequence suggested an important role for the histidines in this region of human PBGS [20]; this has not proven to be the case [21]. Rather, the underlined cysteine residues, which are set in yellow in Figure 3, are seen bound to an active site zinc in human, yeast, and *E. coli* PBGS crystal structures. Replacement of any one of these cysteine residues by alanine via mutagenesis dramatically reduces catalytic activity (E.K.J., unpublished data).

For PBGS that do not have this cysteine-rich site, there is in its place a sequence rich in aspartic acids that was initially identified in pea PBGS [19]. The current analysis shows this aspartate-rich version to have the general sequence DXALDX(Y/F)X_3G(H/Q)DG, and the underlined aspartic acid residues are set in red in Figure 3. The activity of PBGS with the aspartate-rich sequences responds to magnesium and/or potassium, but not to zinc. The first crystal structure of a PBGS with the aspartate-rich sequence, *P. aeruginosa* PBGS (PDB code 1B4K) does not reveal the presence of an active site metal ion [6]. However, the three red aspartic acid

Figure 1. The Crystal Structure of *E. coli* PBGS Showing the Metal Ion Binding Sites that Are Not Phylogenetically Conserved

(A) A stereo diagram showing one dimer of *E. coli* PBGS (PDB code 1L6S) where the protein subunits are shown as a ribbon diagram and colored green and magenta. The active site zinc ions are shown as dark red spheres, and the allosteric magnesium ions are shown as blue spheres. The inhibitor 4,7-dioxosebacic acid is in the active site, carbon atoms are in cyan.

(B) A stereo diagram showing structural details of the active site zinc. The cysteine sulfur atoms are in yellow, and water is a red sphere.

(C) A stereo diagram showing structural details of the allosteric magnesium binding site. Amino acid carbon atoms are colored as per the ribbons in (A). Waters are shown as red spheres. Magnesium is blue, and other atoms are colored by the CPK scheme. The extended ligation network is shown with dashed lines.

The Active Site Residues of Porphobilinogen Synthase sequences available April 2002

NCBI TAXONOMIC CLASSIFICATION	*SPECIES NAME*	ACTIVE SITE AMINO ACIDS, (header is numbered according to human PBGS)
		34 36 50 77 79 120 134 166 170 196 199 209 211 214 216 221 225 250 253 276 282 316 318
EUKARYOTA		
Viridiplantae	*Spinacia oleracea*	P F M V F D V A L D P Y Y Y D G H D G I S P P S D M Y K Y A S S F Y G P F R A L S N P K K T Y Q L V K P P Y Q V S G G E Y L Y
Viridiplantae	*Arabidopsis thaliana*	P F M V F D V A L D P Y S S D G H D G I S P P S D M Y K Y A S S F Y G P F R A L S N P K K T Y Q L V K P P Y Q V S S G E Y L Y
Viridiplantae	*Raphanus sativus*	P F M V F D V A L D P Y S S D G H D G I S P P S D M Y K Y A S S F Y G P F R A L S N P K K T Y Q L V K P P Y Q V S G G E Y L Y
Viridiplantae	*Lycopersicon esculentum*	P F M V F D V A L D P Y S S D G H D G I S P P S D M Y K Y A S S F Y G P F R A L S N P K K T Y Q L V K P P Y Q V S S G E Y L Y
Viridiplantae	*Glycine max*	P F M V F D V A L D P Y S S D G H D G I S P P S D M Y K Y A S S F Y G P F R A L S N P K K T Y Q L V K P P Y Q V S G G E Y L Y
Viridiplantae	*Pisum sativum*	P F M V F D V A L D P Y S S D G H D G I S P P S D M Y K Y A S S F Y G P F R A L S N P K K T Y Q L V K P L Y Q V S G G E Y L Y
Viridiplantae	*Amaranthus tricolor*	M V F D V A L D P Y S S D G H D G I S P P S D M Y K Y A S S F Y G P F R A L S N P K K T Y Q L Y
Viridiplantae	*Hordeum vulgare*	P F M V F D V A L D P Y S S D G H D G I S P P S N M Y K Y A S S F Y G P F R A L S N P K K T Y Q L V K P P Y Q V S G G E Y L Y
Viridiplantae	*Selaginella martensii*	P F M V F D V A L D P Y S S D G H D G I S P P S D M Y K Y A S A F Y E P F R E L S N P K K T Y Q M V K P P Y Q V S S G E Y L Y
Viridiplantae	*Physcomitrella patens*	P F M V F D V A L D P Y S S D G H D G I S P P S D M Y K Y A S A F Y G P S R A L S N P K K T Y Q M V K P P Y Q V S G G E Y L Y
Viridiplantae	*Chlamydomonas reinhardtii*	P F M V F D V A L D P Y N S D G H D G I S P P S D M Y K Y A S A Y Y G P F R A L S A P K K T Y Q M V K P P Y H V S S G E Y L Y
Viridiplantae	*Volvox carteri*	D G H D G I S P P S D M Y K Y A S A Y Y G P F R A L S A P K K T Y Q M V K P P Y H V S S G E Y L Y
Glaucocystophyceae	*Cyanophora paradoxa*	P F M V F D I A L D P Y N S D G H D G I S P P S D M Y K Y A S A Y Y G P F R A L S D P K T T Y Q M V K P P Y Q V S I E Y L Y
Cryptophyta	*Guillardia theta*	G P P S D M Y K Y A S A F Y G P F R A I S A K K R T Y Q M V K P P E Y L Y
Stramenopiles	*Fucus vesiculosus*	P F M V F D V A L D P Y S D Q G H D G V A P P S D M Y K Y A S A F Y G P F R A L S H P K K T Y Q M V K P P Y H V S G G E Y L Y
Stramenopiles	*Laminaria digitata*	P F M V F D V A L D P Y S D Q G H D G V A P P S D M Y K Y A S A F Y G P F R A L S H P K K T Y Q M V K P P Y H V S S G E Y L Y
Stramenopiles	*Odontella sinensis*	P F M V F D V A L D P Y S D Q G H D G V A P P S D M Y K Y A S A Y Y G P F R A L S H P K K T Y Q M V K P P Y H V S G G E Y L Y
Rhodophyta	*Gracilaria gracilis*	M V F D V A L D P Y S D Q G H D G V S P P S D M Y K Y A S A F Y G P F R A L S A P K N T Y Q M V K P P Y H V S S G E Y L Y
Alveolata	*Gonyaulax polyedra*	V F D V A L D P Y N S L G H D G I S P P S D M Y K Y A S A F Y G P F R A L S N P K Q T Y Q M V K P P Y H V S G G E Y L Y
Alveolata	*Plasmodium falciparum*	P F L M F D V A L D P Y N I Y G H D G I C P P S D S Y K Y S S S M Y K P F R I L S N K K Q S Y Q M V K P P L Y
Metazoa; Chordata	*Mus musculus*	P F L L F D V C L C P Y T S H G G H C G G L A P P S D M Y K F A S C F Y G P F R A A S S P R R C Y Q M V K P P Y Q V S G G E F I Y
Metazoa; Chordata	*Homo sapiens*	P F L L F D V C L C P Y T S H G G H C G G L A P P S D M Y K F A S C F Y G P F R A A S S P R R C Y Q M V K P P Y H V S S G E F I Y
Metazoa; Chordata	*Rattus norvegicus*	P F L L F D V C L C P Y T S H G G H C G G L A P P S D M Y K F A S C F Y G P F R A A S S P R R C Y Q M V K P P Y Q V S G G E F I Y
Metazoa; Arthropoda;	*Drosophila melanogaster*	P F M L F D V C I C P Y S S H G G H C G G L A P P S D M Y K F T S N F Y G P F R A A S A P R R C Y Q M V K P P Y Q V S G G E F I Y
Fungi; Ascomycota	*Saccharomyces cerevisiae*	P F L I F D V C L C E Y T S H G G H C G G V A P P S D M Y K F S G N L Y G P F R A A S A P R K C Y Q I V K P P Y H V S S G E Y I Y
Fungi; Ascomycota	*Aspergillus fumigatus*	P F L I F D V C L C E Y T S H G G H C G G I A P P S D M Y K F S G C L Y G P F R A A S C P R R C Y Q M V K P P Y Q V S G G E Y V Y
Fungi; Ascomycota	*Candida glabrata*	P F L I F D V C L C E Y T S H G H C G G V A P P S D M Y K F S G N L Y G P F R A A S S P R K C Y Q I V K P P Y H V S S G E Y I Y
Fungi; Ascomycota	*Schizosaccharomyces pombe*	P F M I F D V C L C E Y T D H G H C G G L S P P S D C Y K F A S G F F G P F R A A G A P R S C Y Q M V K P P Y Q V S G G E F L Y
Fungi; Ascomycota	*Candida albicans*	P F L I F D V C L C E Y T D H G H C G G I A P P S D M Y K F S G N L Y G P F R A A S A P R K A Y Q I V K P P Y H V S S G E Y I Y
ARCHAEA		
Crenarchaeota; Thermoprotei	*Sulfolobus tokodaii*	P F M I F D E C T D E Y T S H G H C G G I A P P S S M Y K Y A S T F Y S P F R A A S K P R R G Y Q M V K P P Y H V S G G E Y I Y
Crenarchaeota; Thermoprotei	*Sulfolobus solfataricus*	P F M I F D E C T D E Y M A N G H C G G L A P P S S M Y K Y A S V M Y G P F R A A S K P R R G Y Q M V K P P Y H V S S G E Y I Y
Crenarchaeota; Thermoprotei	*Pyrobaculum aerophilum*	P F M I F D V C L C E Y T E H G H C G G V A P P S G M Y K Y A S A F Y G P F R A A S A P R R T Y Q M V K P P Y N V S G G E Y L Y
Crenarchaeota; Thermoprotei	*Aeropyrum pernix*	P F L L F D V C L C G Y T D H G H C G G Y A P P S G M Y K Y A S G F Y G P F R V M S A P R R S Y Q M V K P P Y N V S S G E Y I Y
Euryarchaeota; Thermoplasmata	*Thermoplasma volcanium*	P F M L F D L C L C E Y T D T G Q C G G L A P P S G M Y K F S S N L Y G P F R A A S A P R K S Y Q M V K P P Y S V S G G E Y I Y
Euryarchaeota; Thermoplasmata	*Ferroplasma acidarmanus*	P F M I F D L C L C E Y T D T G H C G G V A P P S G M Y K F A S N L Y G P F R A A S T P R K S Y Q M V K P P Y M V S S G E Y I Y
Euryarchaeota; Thermoplasmata	*Thermoplasma acidophilum*	P F M L F D L C L C E Y T D T G Q C G G L A P P S G M Y K F S S N L Y G P F R A A S A P R K S Y Q M V K P P Y S V S G G E Y I Y
Euryarchaeota; Methanobacteria	*Methanothermus sociabilis*	P F M L F D V C L C Q Y T E H G H C G G I A P P S D M Y K Y A S S F Y E P F R A V S S P R S T Y Q M V K P P Y N V S S G E Y I H
Euryarchaeota; Methanobacteria	*Methanothermobacter thermautotrophicus*	P F M L F D V C L C Q Y T S H G H C G G I A P P S D M Y K Y A S A F Y A P F R A V S A P R R S Y Q M V K P P Y N V S G G E Y I H
Euryarchaeota; Archaeoglobi	*Archaeoglobus fulgidus*	P F M I F D V C L C E Y T T H G H C G G V A P P S G M Y K Y A S N F Y S P F R A A S G F R R G Y Q M V K P P Y N V S G G E Y I Y
Euryarchaeota; Halobacteria	*Halobacterium sp. NRC-1*	P F M V F D V C L C E Y T S H G H C G G V A P P S A M Y K Y E S A F Y G P F R A A G A P R R H Y Q M V K P P Y N V S S G E Y I Y
Euryarchaeota; Methanococci	*Methanococcus jannaschii*	P F M I F D C C L C E Y T S H G H C G G I A P P S D M Y K Y A S S F Y G P F R A A S A P R K S Y Q L V K P P Y C V S G G E Y I Y
Euryarchaeota; Methanococci	*Methanosarcina barkeri*	P F M I F D V C M C E Y T S H G H C G G I A P P S C M Y K Y H S C F Y G P F R A A S G Y R S T Y Q I V K P P Y N V S S G E Y I Y
EUBACTERIA		
Firmicutes; Actinobacteria	*Streptomyces coelicolor A3(2)*	P F M M F D L C L D E F T D H G H C G V G P P S G M Y K Y A S A F Y G P F R A V S S L R K T Y Q M V K P P Y Q I S G G E Y L Y
Firmicutes; Actinobacteria	*Propionibacterium freudenreichii subsp. s*	P F M M F D V C L D E F T D H G H C G V G P P S G M Y K Y A S G F F G P F R A V S Q L R R A Y Q M V K P P Y V V S G G E Y V Y
Firmicutes; Actinobacteria	*Mycobacterium tuberculosis H37Rv*	P F M M F D T C L D E F T D H G H C G V G P P S G M Y K F A S A F Y G P F R A V S S L R R T Y Q M V K P P Y Q V S G G E Y L Y
Firmicutes; Actinobacteria	*Mycobacterium avium*	P F M M F D T C L D E F T D H G H C G V G P P S G M Y K F A S A F Y G P F R A V S S L R R T Y Q M V K P P Y Q V S G G E Y L Y
Firmicutes; Actinobacteria	*Mycobacterium leprae*	P F M N F D T C L D E F T D H G H C G V G P P S G M Y K F S S A F Y G P F R A V S C S R R T Y Q M I K P P Y Q V S G G E Y F Y
Firmicutes; Actinobacteria	*Mycobacterium bovis*	P F M M F D T C L D E F T D H G H C G V G P P S G M Y K F A S A F Y G P F R A V S S L R R T Y Q M V K P P Y Q V S G G E Y L Y
Firmicutes; Actinobacteria	*Mycobacterium smegmatis*	P F M M F D T C L D E F T D H G H C G V G P P S G M Y K F A S A F Y G P F R A V S S L R R T Y Q M V K P P Y Q I S G G E Y L Y
Firmicutes; Actinobacteria	*Corynebacterium diphtheriae*	P F M D F D T C L D E F T D H G H C G G I S P P S G M Y K Y A S A F Y G P F R A V S S L R R A Y Q M V K P P Y Q V S S G E Y L Y
Firmicutes; Bacillus/Clostridium group	*Staphylococcus epidermidis*	P F L M F D T C L C E Y T D H G H C G G V A P P S N M Y K Y A S S F F G P F R A A S A P R K T Y Q I V K P P Y N V S G G E Y I Y
Firmicutes; Bacillus/Clostridium group	*Staphylococcus aureus*	P F L M F D T C L C E Y T D H G H C G G V A P P S N M Y K Y A S S F F G P F R A A S A P R K T Y Q I V K P P Y N V S G G E Y I Y
Firmicutes; Bacillus/Clostridium group	*Bacillus subtilis*	P F M I F D T C L C E Y T D H G H C G G L A P P S N M Y K Y S S E F Y G P F R A A S T P R K T Y Q I V K P P Y N V S G G E Y I Y
Firmicutes; Bacillus/Clostridium group	*Bacillus halodurans*	P F M I F D T C L C Q F T D H G H C G G V A P P S N M Y K Y A S A F Y G P F R A A S S P R K T Y Q I V K P P Y N V S G G E Y L Y
Firmicutes; Bacillus/Clostridium group	*Bacillus anthracis*	P F M I F D T C L C Q F T S H G H C G G V A P P S N M Y K Y S S A F Y G P F R A A G A P R K T Y Q I V K P P Y N V S G G E Y I Y
Firmicutes; Bacillus/Clostridium group	*Geobacillus stearothermophilus*	P F M M F D T C L C E Y T S H G H C G G V A P P S N M Y K Y A S A F Y G P F R A A S A P R K T Y Q M V K P P Y N V S G G E Y I Y
Firmicutes; Bacillus/Clostridium group	*Listeria innocua*	P F M I F D T C L C E F T D H G H C G G V A P P S N M Y K Y A S A F Y G P F R A A S A P R K S Y Q I V K P P Y N V S S G E Y I Y
Firmicutes; Bacillus/Clostridium group	*Listeria monocytogenes EGD-e*	P F M I F D T C L C E F T D H G H C G G V A P P S N M Y K Y A S A F Y G P F R A A S A P R K S Y Q I V K P P Y N V S G G E Y I Y
Firmicutes; Bacillus/Clostridium group	*Desulfitobacterium hafniense*	P F M L F D V C L C E Y T D H G H C G G V A P P S D M Y K F A S A F Y G P F R A A S A P R R T Y Q I V K P P Y N V S S G E Y I Y
Firmicutes; Bacillus/Clostridium group	*Selenomonas ruminantium*	P F M E F D V C M C E Y T D H G H C G G H A P P S D M Y K Y A S G Y Y G P F R A A S A P R R Q Y Q M V K P P Y N V S G G E Y I Y
Firmicutes; Bacillus/Clostridium group	*Clostridium botulinum*	P F L M F D V C M C Q Y T S H G H C G G I A P P S D M Y K Y C S A F Y G P F R A A S A P R K T Y Q M V K P P Y N V S S G E Y I Y
Firmicutes; Bacillus/Clostridium group	*Clostridium difficile*	P F L M F D V C M C Q Y T S H G H C G G I A P P S D M Y K Y A S N Y Y G P F R A A S A P R K T Y Q M V K L P Y N V S G G E Y I Y
Firmicutes; Bacillus/Clostridium group	*Clostridium josui*	P F L L F D I C M C E Y T S H G H C G G I A P P S D M Y K Y A S S F Y G P F R A A
Firmicutes; Bacillus/Clostridium group	*Clostridium acetobutylicum*	P F L I F D V C M C E Y T S H G H C G G I A P P S D M Y K Y C S A F Y G P F R A A S A P R K S Y Q M V K P P Y S V S S G G E Y I Y
Firmicutes; Bacillus/Clostridium group	*Clostridium perfringens*	P F L I F D V C M C E Y T S H G H C G G I A P P S D M Y K Y C S A F Y G P F R A A S A P R K T Y Q M V K P P Y N V S S G E E F I Y
Aquificae	*Aquifex aeolicus*	P F M I F D V C F C E Y T T H G H C G G V A P P S G M Y K F A S A Y Y G P F R A A S A P R R T Y Q M V K P P Y N V S S G E Y I Y
Thermus/Deinococcus group	*Deinococcus radiodurans*	P F M I F D T C L C E Y T S H G H C G G H A P P S A M Y K Y A S A Y Y G P F R A A S A P R A S Y Q M V K P P Y N V S S G E Y I Y

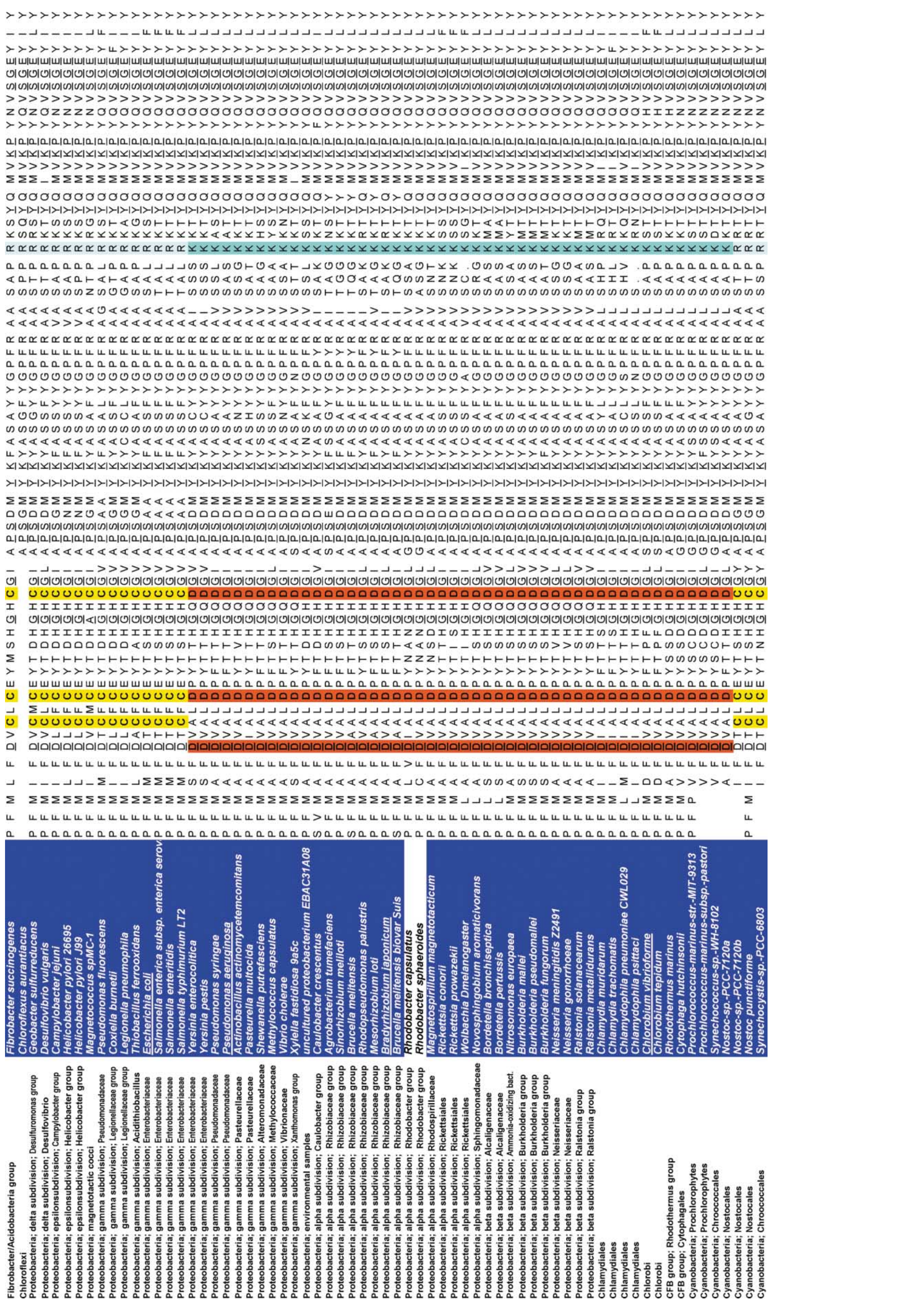

residues in Figure 3 are oriented to form a metal ion binding site, as illustrated in Figure 4A. An ion in this position would not be in the same location as the zinc ion seen bound to the cysteine-rich sequence, which is consistent with the notion that there may be phylogenetic variations in the PBGS-catalyzed reaction mechanism [22]. A very recent *P. aeruginosa* PBGS crystal structure (PDB code 1ZGZ) shows sodium associated with the red aspartic acid residues, as illustrated in Figure 4B [7]. Figure 4C is a structure overlay of the metal binding region of the cysteine-rich human PBGS (PDB code 1E51) and *E. coli* PBGS (PDB code 1L6S) with the aspartate-rich *P. aeruginosa* PBGS (PDB codes 1B4K and 1ZGZ). The human PBGS structure contains the product porphobilinogen at the active site; the *E. coli* PBGS contains the inhibitor 4,7-dioxosebacic acid; the *P. aeruginosa* PBGS structures contain the inhibitors levulinic acid and 5-fluorolevulinic acid at the active site. There are no crystal structures yet available for a PBGS whose kinetic properties suggest an active site magnesium ion (e.g., *B. japonicum* [13] or *P. sativum* [pea] [14]).

For all PBGS, we find a strict correlation between the active site metal binding sequence and a basic active site residue that is part of a mobile lid that gates access to the active site. This basic residue is approximately 100 amino acids toward the C terminus relative to the metal binding sequence. The cysteine-rich active site metal binding sequence correlates with arginine (light blue in Figure 3), and the aspartate-rich sequence correlates with lysine (turquoise in Figure 3) at this position. The basic residues are highlighted in the sequences shown in Figure 3 and included in the structure illustrations of Figure 4.

The Allosteric Magnesium Binding Sequence

Details of the allosteric magnesium binding site of *E. coli* PBGS are illustrated in Figure 1C. This octahedral site contains only one amino acid (Glu231) that contributes to the first coordination sphere of the magnesium. The remainder of the five first coordination sphere ligands are water molecules. Outer sphere ligands include additional water molecules, two invariant aspartate residues, two backbone carbonyls, and an arginine that derives from the N-terminal arm of an adjacent subunit. The determinants for allosteric magnesium binding in the sequence $\underline{R}X_{\sim 164}DX_{\sim 65}\underline{E}XXXD$ are the underlined residues, which correspond to Arg11 and Glu231 in Figure 1C, and are used to determine the presence or absence of this metal ion in PBGS. Many PBGS that lack the magnesium ligands contain instead the analogous sequence ($XX_{\sim 164}DX_{\sim 65}XXX\underline{R}D$) where the underlined arginine residue contains a guanadinium moiety that is spatially equivalent to the allosteric magnesium [23]. Species names on blue background in Figure 3 indicate the presence of the allosteric magnesium as do the colors green and magenta in Figures 2 and 5. Prior studies showed that the allosteric magnesium of *E. coli* PBGS causes a reduction in the K_m for substrate, an increase in V_{max}, and that magnesium and substrate cooperatively enhance the stability of the octameric quaternary structure [12].

The Phylogenetic Distribution of the Active Site Metal Binding Sequence of PBGS

The phylogenetic distribution of PBGS active site residues is detailed in Figure 3 and summarized in Figure 5. The data, described below, shed light on the metal binding sequences of the primordial PBGS and on the advent of the current variation in these sequences.

The cysteine-rich metal binding sequence (yellow and green in Figure 5, according to the color code in Figure 2) is present in all archaea, some bacteria, and some eucarya. The exclusive existence of a zinc binding domain in one of the three major branches of life (the archaea) suggests that the cysteine-rich PBGS represents the primordial PBGS. Among bacterial species, approximately one-half of the PBGS contain the cysteine-rich sequence. These include the PBGS from the Gram-positive bacteria (firmicutes) and single examples of the Thermus/Deinococcus group and the aquificales. Available PBGS sequences from the δ- and ϵ-proteobacteria have the cysteine-rich domain. Among the eucarya, animals (metazoa), and yeast have the cysteine-rich PBGS.

In contrast, the aspartate-rich active site metal binding sequence of PBGS (red and magenta in Figure 5) is not found in the archaea. Bacterial species with the aspartate-rich sequence include the α- and β-proteobacteria, the CFB group, chlorobi, and chlamydiales. Among the eucarya, the photosynthetic organisms (plants, mosses, and algae) and the available sequences from protists have the aspartate-rich PBGS sequence.

Several groups of bacteria contain examples of both zinc-utilizing and non-zinc PBGS. As stated above, some subclasses of proteobacteria (δ and ϵ) have the cysteine-rich domain, while others (α and β) have the aspartate-rich domain. This mixture also exists within the subclass known as the γ-proteobacteria. In fact, even members of the same family of γ-proteobacteria show differences (e.g., the enterobacteriacea *Salmo-*

Figure 3. A Taxonomic-Based Sequence Alignment of the Active Site Residues of PBGS

The amino acids that comprise the active site are considered to be residues within 8 Å of porphobilinogen in human PBGS crystal structure (PDB code 1E51) and an unpublished *E. coli* PBGS structure that also contains enzyme-bound product. Residues are numbered vertically across the top according to human PBGS. Asterisks are placed above the columns of residues that are not within 8 Å of product. Underlined residues are universally conserved. The yellow cysteines define the ligands to the active site zinc of some PBGS. The red aspartate residues form a putative metal binding site in those PBGS that do not use an active site zinc. There is a lysine (turquoise) or arginine (light blue) that cosegregate respectively with the absence or presence of the active site zinc binding site. Species names on a blue background correspond to the PBGS whose sequences indicate a binding site for the allosteric magnesium ion. Underlined species names indicate those PBGS that have been purified and characterized with respect to their metal ion requirements [11–18].

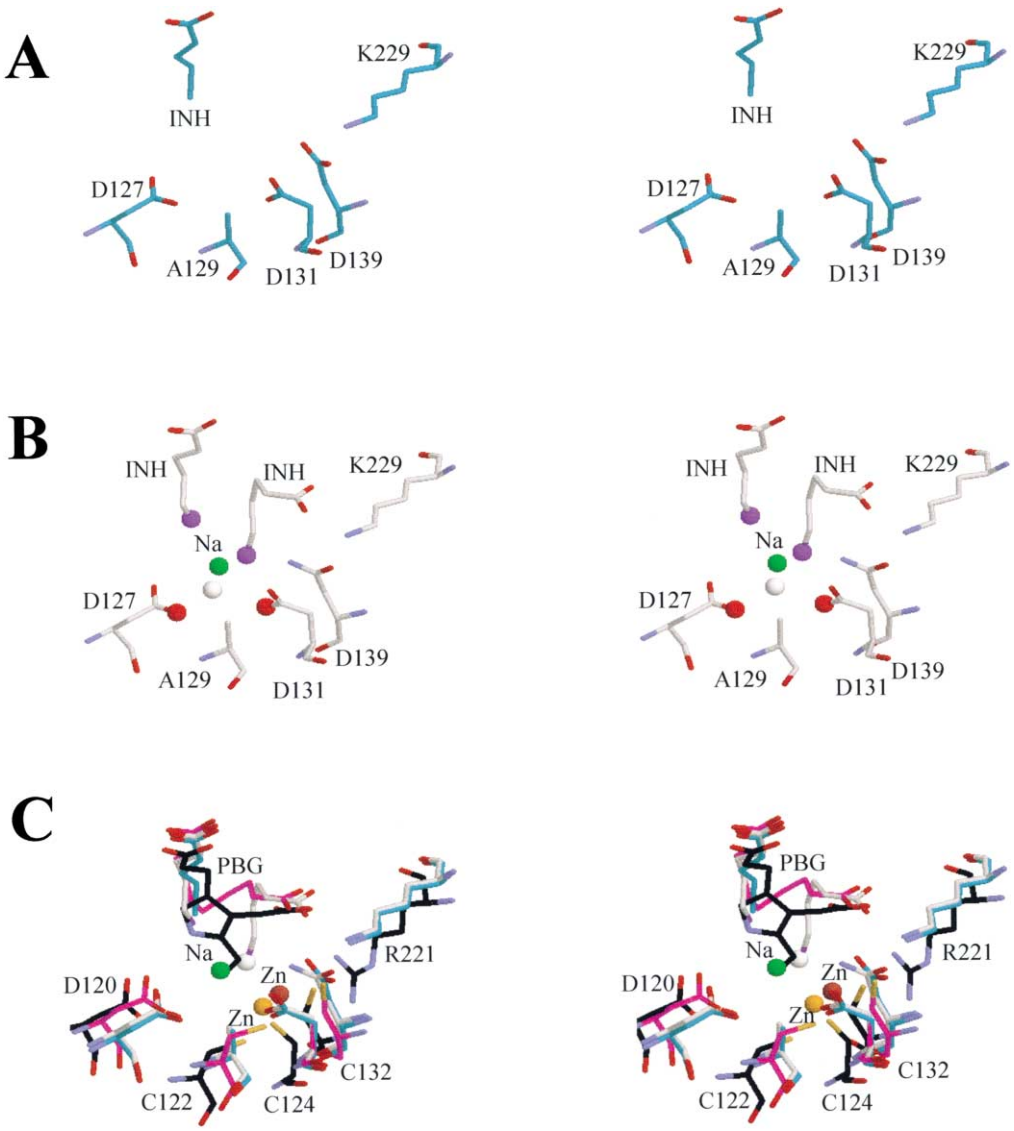

Figure 4. Comparative Views of the PBGS Active Site Metal Binding Region

(A) A stereo diagram of the active site of *P. aeruginosa* PBGS (PDB code 1B4K), where the carbon atoms are colored cyan and the inhibitor (INH) is levulinic acid, which has formed a Schiff base linkage to an active site lysine (data not shown). Oxygen and nitrogen atoms are colored CPK.

(B) A stereo diagram of *P. aeruginosa* PBGS (PDB code 1ZGZ), where the carbon atoms are colored gray and there are two molecules of the inhibitor (INH) 5-fluorolevulinic acid, which have both formed Schiff base linkages to active site lysines (data not shown). The sodium atom (green) and its ligands are depicted as balls where carboxyl oxygens are red, water is white, and fluorine is purple.

(C) A stereo overlay of structures 1B4K (described in [A] above), 1ZGZ (described in [B] above), with human PBGS (PDB code 1E51), which is labeled. The carbon atoms of 1E51 are colored black and the active site contains the product porphobilinogen (PBG). The active site zinc in 1E51, illustrated as an orange ball, is liganded to the three cysteine sulfur atoms and the free amino group of porphobilinogen. The amino group of porphobilinogen is not readily visible because it is nearly coincident with the sodium ion of 1ZGZ (green). ^{13}C NMR data support the notion that the environment of enzyme-bound product is different for the PBGS that contain an active site zinc and those that do not (e.g., [18, 33]). The final structure illustrated is *E. coli* PBGS (PDB code 1L6S), which is also illustrated in Figure 1. The carbon atoms are magenta, the inhibitor is 4,7-dioxosebacic acid which has formed a di-Schiff base to the active site lysine residues (data not shown). The zinc is a dark red ball, and the water ligand is shown as a white ball, which is nearly coincident with a fluorine atom from structure 1ZGZ (shown in [B] above). This overlay shows significant variation in the positions of some of the amino acids, the metal ions, and the product/inhibitors, which may represent some aspects of the motion that is required in the condensation of two molecules of the substrate 5-aminolevulinic acid to the product porphobilinogen.

nella versus *Yersinia*). The cyanobacteria also contain examples of both types of PBGS active sites and this is discussed in more detail below.

Finally, it is interesting to note that the Gram-positive actinobacteridae and the archaeal crenarcheoteon *Sulfolobus* are the only organisms that have a hybrid metal binding sequence DXCLDX(Y/F)X_3G(H/Q)CG. These species of PBGS contain arginine as the basic residue that segregates with the active site metal binding sequence, and the proteins are presumed to be zinc dependent.

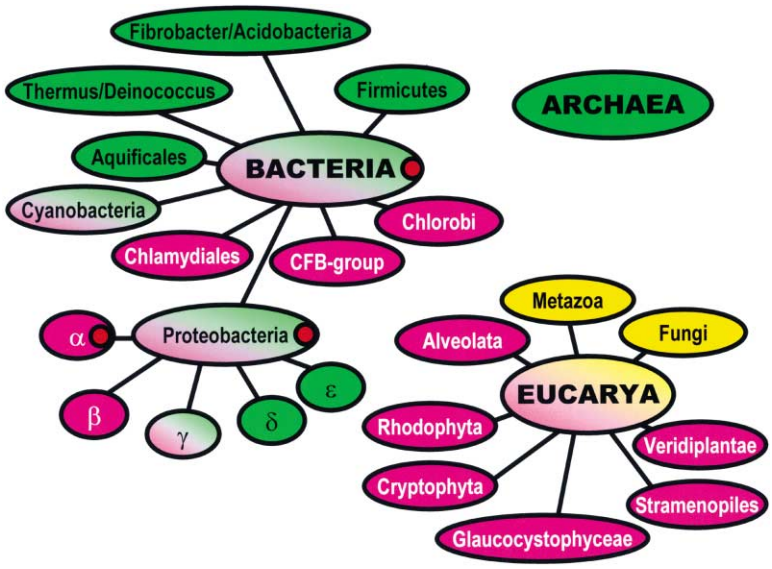

Figure 5. The Phylogenetic Distribution of Metal Binding Properties of PBGS

The coloring follows that of the four quadrants of Figure 2. The organization of this figure reflects a taxonomic hierarchy and is not intended to imply evolutionary distance. The PBGS of the *Rhodobacter* family of α-proteobacteria are the only ones that fall in the red quadrant of Figure 2.

The Phylogenetic Distribution of the Allosteric Magnesium Binding Sequence of PBGS

The allosteric magnesium binding determinants are found in almost all PBGS except for the eucarya metazoa (animals) and yeast, which appear in yellow in Figures 2 and 5. These PBGS, which uniformly lack the magnesium ligands, contain the spatially equivalent compensating arginine. They also contain the binding site for a second zinc, previously called ZnA, which is near the active site, but is not essential for activity [10]. All archaeal and almost all bacterial PBGS contain the binding determinants for the allosteric magnesium (green and magenta in Figures 2 and 5). The only exceptions seen to date are found in the bacterial genus *Rhodobacter* (*R. capsulatus* and *R. spheroids*), which respectively contain asparagine and leucine in place of the first coordination sphere glutamate, and are in the red quadrant of Figure 2 and are shown in red in Figure 5. The *Rhodobacter* PBGS lack the allosteric magnesium but contain the compensating positive charge from arginine found in metazoan and yeast PBGS. It is ironic that PBGS from *Rhodobacter* was initially characterized as generally representative of PBGS from photosynthetic organisms [24, 25]. Two additional α-proteobacteria, *Agrobacterium tumefaciens* and *Sinorhizobium meliloti*, contain PBGS with aspartic acid in place of the first coordination sphere glutamate.

Hypotheses Concerning the Evolution of the Active Site Metal of PBGS

A functional active site metal binding sequence is essential for PBGS activity, which in turn is essential for most cellular life. The distribution of PBGS sequences throughout evolution argues against a gradual drift in a single gene that morphed from the cysteine-rich to the aspartate-rich metal binding sequence. A teleologic rationale for the distribution of active site metal ion usage by PBGS can be found in a necessary step in chlorophyll biosynthesis, which is the thermodynamically difficult insertion of magnesium into the planar and nitrogen-rich tetrapyrrole core. This unfavorable reaction is in direct competition with the spontaneous insertion of zinc into protoporphyrin IX [26]. This thermodynamic quandary is lessened if chlorophyll biosynthesis is carried out in the presence of high concentrations of free magnesium and very low concentrations of free or labile zinc. In fact, the concentration of magnesium in chloroplasts during active chlorophyll biosynthesis is about 10 mM [27]. Thus, the thermodynamic difficulty of inserting magnesium into protoporphyrin IX could provide the evolutionary pressure against a chlorophyll biosynthetic enzyme (e.g., PBGS) whose activity is dependent upon zinc. This rationale was originally put forth for PBGS that function in chloroplasts, all of which have the aspartate-rich metal binding sequence [28]. The rationale is now extended to the photosynthetic α-proteobacteria as well as the photosynthetic green sulfur bacteria (chlorobi), which also have the aspartate-rich metal sequence.

It is noteworthy that the cyanobacteria, in which oxygenic photosynthesis is believed to have first appeared, do not all contain a PBGS with the aspartate-rich sequence. Of the seven cyanobacterial PBGS sequences available, only four have the aspartate-rich sequence. Most interesting is the completed genome of *Nostoc* (formerly Anabaena) *sp. PCC 7120*, which is the only species yet documented to contain *both* types of PBGS in a single genome. There are two copies of the PBGS, one with the cysteine-rich metal binding sequence and one with the aspartate-rich metal binding sequence. The chromosomal orientation of these genes suggests a gene duplication event wherein the aspartate-rich sequence might have evolved through functionally impotent forms in the presence of a functional gene with the cysteine-rich domain. Alternatively, the second gene may have arisen through a horizontal gene transfer. The presence of two PBGS encoding genes in cyanobacteria is significant not only because the cyanobacteria are cited as the first organisms to develop oxygenic photosynthesis, but also because these microorganisms are believed to be the endosymbiotic precursors to chloro-

plasts. The cyanobacteria PBGS sequence data contribute to the recently reviewed debate on the complex evolution of photosynthesis [29].

What then of the nonphotosynthetic bacterial PBGS that have the aspartic acid-rich metal binding sequence? Known crystal structures and the current sequence analyses show that these PBGS uniformly have the allosteric metal binding site, which is specific for magnesium. This allosteric magnesium resides outside the active site and has a dissociation constant that is approximately two orders of magnitude weaker than the catalytically essential magnesium that is believed to bind to the aspartate-rich active site metal binding sequence (e.g., [13]). In the event that a bacterial PBGS were to acquire the aspartate-rich sequence, it might be inconsequential since these PBGS already have a weaker binding magnesium.

Unanswered Questions about the Variation in PBGS Sequence, Structure, and Function

The current work analyses the phylogenetic segregation of two variable properties of the PBGS by documenting the determinants for an active zinc and an allosteric magnesium. Remaining questions include the location of magnesium at the enzyme active site and the complex and variable interactions between magnesium and potassium in PBGS such as that of *B. japonicum* [13].

The current sequence analysis does not shed light on the determinants for variation in metal ion stoichiometry. For instance, there are extensive data on some PBGS that indicate half-site metal binding along with half-site reactivity. Human PBGS is one example where studies indicate the homo-octameric protein binds four zinc atoms at the catalytic site (previously called ZnB) and four zinc ions at a neighboring site (previously called ZnA) whose function is less clear [10]. The crystal structures of human PBGS and *P. aeruginosa* PBGS show significant asymmetry in the PBGS dimer, which constitutes the asymmetric unit of the crystal. These structures (PDB codes 1E51 and 1B4K) show half-sites metal binding for the catalytic zinc and the allosteric magnesium, respectively. They also show significant disorder in the subunit that is devoid of metal ion. In contrast, crystal structures of yeast PBGS contain the monomer in the asymmetric unit (e.g., PDB codes 1AW5 and 1YLV). One deposited structure for *E. coli* PBGS shows a monomeric asymmetric unit (PDB code 1B4E), while others show a dimer that is only slightly asymmetric (PDB codes 1I8J, 1L6S, and 1L6Y). Hence, the sequence determinants for dimer asymmetry and half-sites metal binding/reactivity remain to be clarified.

Interestingly, the current study revealed that several completed genomes lack PBGS. These genomes were explicitly searched for and uniformly found to lack evidence of either of two alternate pathways that make the PBGS substrate 5-aminolevulinic acid, as well as the next enzyme in the common tetrapyrrole pathway, porphobilinogen deaminase. Some of these organisms are parasites, which discard inessential biosynthetic pathways [30]. Others, such as the Lactococci, are known to grow fermentatively in the absence of endogenous heme [31]. However, one, the eukaryotic *Caenorhabditis elegans* (the common soil roundworm), was a surprise, as this organism requires heme. *C. elegans* must therefore get all tetrapyrroles nutritionally.

Significance

PBGS activity is necessary for the de novo biosynthesis of the tetrapyrrole pigments that are essential to methanogens, photosynthetic organisms, and organisms that require the multiple functions of heme. PBGS is unique in its variation of active site and allosteric metal ions. Of particular interest is a variation in the chemically dissimilar zinc, magnesium, and potassium at the enzyme active site. The current analysis of PBGS sequences and crystal structures has enhanced definition of the active site metal binding sequence. Distillation of the metal binding sequences allows us to segregate the PBGS into four main groups on the basis of whether or not they require an active site zinc and whether or not they use an allosteric magnesium. We determine the phylogenetic distribution of these groups, and contribute to the growing body of molecular data that address the forces that might have driven evolutionary changes in proteins. The phylogenetic distribution of the PBGS suggests that the zinc-requiring form existed in earliest life forms, prior to the rise in atmospheric oxygen. The data support a hypothesis that the thermodynamic difficulty of incorporating magnesium into a chlorophyll precursor provided the evolutionary driving force for the loss of the active site zinc of PBGS. A possible gene duplication event in cyanobacteria provides a mechanism for the appearance of PBGS that does not require a catalytic zinc. In contrast, the allosteric magnesium binding site is present in more than 90% of the PBGS sequences including all archaea, many eucarya, and all but the *Rhodobacter* genus of bacteria. For reasons that remain cryptic, the allosteric magnesium is absent in PBGS from metazoa and yeast, which contain a second zinc binding site. There is no obvious spatial or functional correlation between ZnA and MgC.

Experimental Procedures

PBGS sequences were collected by carrying out a series of Blast and PSIBLAST searches [32] using spinach PBGS as the query. Databases included nonredundant GenBank (www.ncbi.nlm.nih.gov/blast/index.html) as well as multiple individual genome databases available courtesy of and through links from The Institute for Genome Research (www.tigr.org). The sequences were initially aligned using the GCG program Pileup. The alignment was exported to EXCEL for refinement and annotation. Taxonomy annotation was added manually according to the NCBI classifications (www.ncbi.nlm.nih.gov/Taxonomy/taxonomyhome.html). The aligned and annotated sequences were then sorted and clustered manually according to taxonomy. The data were then culled to include only those amino acids at the PBGS active site and those associated with the allosteric magnesium. For the purpose of this analysis, the amino acids that constitute the PBGS active site are arbitrarily defined as those within 8 Å of the product porphobilinogen in the human PBGS crystal structure, PDB code 1E51 (N.L. Mills-Davies, submitted). These residues are the same as those within 8 Å of porphobilinogen bound to *E. coli* PBGS (H.L. Carrell, personal communication).

Acknowledgments

The author acknowledges Drs. Samuel Beale (Brown University) and Erica Golemis (FCCC) for helpful discussion. This work was supported by NIH grants ES03654 (E.K.J.) and CA06927 (ICR), and by an appropriation from the Commonwealth of Pennsylvania. The FCCC Research Information Technology and Research Secretarial Services Facilities were used in the preparation of this manuscript.

Received: August 16, 2002
Revised: October 31, 2002
Accepted: November 11, 2002

References

1. Shemin, D., and Russell, C.S. (1953). Delta-aminolevulinic acid, its role in the biosynthesis of porphyrins and purines. J. Am. Chem. Soc. *75*, 4873.
2. Bock, C.W., Katz, A.K., and Glusker, J.P. (1995). Hydration of zinc ions: a comparison with magnesium and beryllium ions. J. Am. Chem. Soc. *117*, 3754–3765.
3. Erskine, P.T., Senior, N., Awan, S., Lambert, R., Lewis, G., Tickle, I.J., Sarwar, M., Spencer, P., Thomas, P., Warren, M.J., et al. (1997). X-ray structure of 5-aminolaevulinate dehydratase, a hybrid aldolase. Nat. Struct. Biol. *4*, 1025–1031.
4. Erskine, P.T., Newbold, R., Brindley, A.A., Wood, S.P., Shoolingin-Jordan, P.M., and Warren, M.J. (2001). The X-ray structure of yeast 5-aminolaevulinic acid dehydratase complexed ith substrate and three inhibitors. J. Mol. Biol. *312*, 133–141.
5. Kervinen, J., Jaffe, E.K., Stauffer, F., Neier, R., Wlodawer, A., and Zdanov, A. (2001). Mechanistic basis for suicide inactivation of porphobilinogen synthase by 4,7-dioxosebacic acid, an inhibitor that shows dramatic species selectivity. Biochemistry *40*, 8227–8236.
6. Frankenberg, N., Erskine, P.T., Cooper, J.B., Shoolingin-Jordan, P.M., Jahn, D., and Heinz, D.W. (1999). High resolution crystal structure of a Mg^{2+}-dependent porphobilinogen synthase. J. Mol. Biol. *289*, 591–602.
7. Frere, F., Schubert, W.D., Stauffer, F., Frankenberg, N., Neier, R., Jahn, D., and Heinz, D.W. (2002). Structure of porphobilinogen synthase from *Pseudomonas aeruginosa* in complex with 5-fluorolevulinic acid suggests a double Schiff base mechanism. J. Mol. Biol. *320*, 237–247.
8. Jaffe, E.K., and Hanes, D. (1986). Dissection of the early steps in the porphobilinogen synthase-catalyzed reaction: requirements for Schiff's base formation. J. Biol. Chem. *261*, 9348–9353.
9. Warren, M.J., Cooper, J.B., Wood, S.P., and Shoolingin-Jordan, P.M. (1998). Lead poisoning, haem synthesis and 5-aminolaevulinic acid dehydratase. Trends Biochem. Sci. *23*, 217–221.
10. Jaffe, E.K., Martins, J., Li, J.M., Kervinen, J., and Dunbrack, R.L., Jr. (2001). Molecular mechanism of lead inhibition of human porphobilinogen synthase. J. Biol. Chem. *276*, 1531–1537.
11. Jaffe, E.K., Volin, M., Bronson-Mullins, C.R., Dunbrack, R.L., Jr., Kervinen, J., Martins, J., Quinlan, J.F., Jr., Sazinsky, M.H., Steinhouse, E.M., and Yeung, A.T. (2000). An artificial gene for human porphobilinogen synthase allows comparison of an allelic variation implicated in susceptibility to lead poisoning. J. Biol. Chem. *275*, 2619–2626.
12. Jaffe, E.K., Ali, S., Mitchell, L.W., Taylor, K.M., Volin, M., and Markham, G.D. (1995). Characterization of the role of the stimulatory magnesium of *Escherichia coli* porphobilinogen synthase. Biochemistry *34*, 244–251.
13. Petrovich, R.M., Litwin, S., and Jaffe, E.K. (1996). *Bradyrhizobium japonicum* porphobilinogen synthase uses two Mg(II) and monovalent cations. J. Biol. Chem. *271*, 8692–8699.
14. Kervinen, J., Dunbrack, R.L., Jr., Litwin, S., Martins, J., Scarrow, R.C., Volin, M., Yeung, A.T., Yoon, E., and Jaffe, E.K. (2000). Porphobilinogen synthase from pea: expression from an artificial gene, kinetic characterization, and novel implications for subunit interactions. Biochemistry *39*, 9018–9029.
15. Senior, N.M., Brocklehurst, K., Cooper, J.B., Wood, S.P., Erskine, P., Shoolingin-Jordan, P.M., Thomas, P.G., and Warren, M.J. (1996). Comparative studies on the 5-aminolaevulinic acid dehydratases from *Pisum sativum*, *Escherichia coli* and *Saccharomyces cerevisiae*. Biochem. J. *320*, 401–412.
16. Rhie, G., Avissar, Y.J., and Beale, S.I. (1996). Structure and expression of the Chlorobium vibrioforme hemB gene and characterization of its encoded enzyme, porphobilinogen synthase. J. Biol. Chem. *271*, 8176–8182.
17. Frankenberg, N., Heinz, D.W., and Jahn, D. (1999). Production, purification, and characterization of a Mg^{2+}-responsive porphobilinogen synthase from *Pseudomonas aeruginosa*. Biochemistry *38*, 13968–13975.
18. Frankenberg, N., Jahn, D., and Jaffe, E.K. (1999). *Pseudomonas aeruginosa* contains a novel type V porphobilinogen synthase with no required catalytic metal ions. Biochemistry *38*, 13976–13982.
19. Boese, Q.F., Spano, A.J., Li, J.M., and Timko, M.P. (1991). Aminolevulinic acid dehydratase in pea (*Pisum sativum L.*). Identification of an unusual metal-binding domain in the plant enzyme. J. Biol. Chem. *266*, 17060–17066.
20. Wetmur, J.G., Bishop, D.F., Cantelmo, C., and Desnick, R.J. (1986a). Human delta-aminolevulinate dehydratase: nucleotide sequence of a full-length cDNA clone. Proc. Natl. Acad. Sci. USA *83*, 7703–7707.
21. Mitchell, L.W., Volin, M., and Jaffe, E.K. (1995). The phylogenetically conserved histidines of *Escherichia coli* porphobilinogen synthase are not required for catalysis. J. Biol. Chem. *270*, 24054–24059.
22. Jaffe, E.K., Kervinen, J., Martins, J., Stauffer, F., Neier, R., Wlodawer, A., and Zdanov, A. (2002). Species-specific inhibition of porphobilinogen synthase by 4-oxosebacic acid. J. Biol. Chem. *277*, 19792–19799.
23. Jaffe, E.K. (2000). The porphobilinogen synthase family of metalloenzymes. Acta Crystallogr. D *56*, 115–128.
24. Nandi, D.L., Baker-Cohen, K.F., and Shemin, D. (1968). Delta-aminolevulinic acid dehydratase of *Rhodopseudomonas spheroides*. J. Biol. Chem. *243*, 1224–1230.
25. Nandi, D.L., and Shemin, D. (1973). Delta-aminolevulinic acid dehydratase of *Rhodopseudomonas capsulata*. Arch. Biochem. Biophys. *158*, 305–311.
26. Baum, S.J., and Plane, R.A. (1966). Kinetics of the incorporation of magnesium(II) into porphyrin. J. Am. Chem. Soc. *88*, 910–913.
27. Walker, D.A. (1976). Regulatory mechanisms in photosynthetic carbon metabolism. Curr. Top. Cell. Regul. *11*, 203–241.
28. Jaffe, E.K. (1995). Porphobilinogen synthase, the first source of heme's asymmetry. J. Bioenerg. Biomembr. *27*, 169–179.
29. Xiong, J., and Bauer, C.E. (2002). Complex evolution of photosynthesis. Annu. Rev. Plant Biol. *53*, 503–521.
30. Andersson, J.O., and Andersson, S.G. (1999). Insights into the evolutionary process of genome degradation. Curr. Opin. Genet. Dev. *9*, 664–671.
31. Duwat, P., Sourice, S., Cesselin, B., Lamberet, G., Vido, K., Gaudu, P., LeLoir, Y., Violet, F., Loubiere, P., and Gruss, A. (2001). Respiration capacity of the fermenting bacterium *Lactococcus lactis* and its positive effects on growth and survival. J. Bacteriol. *183*, 4509–4516.
32. Altschul, S.F., Madden, T.L., Schäffer, A.A., Zhang, J., Zhang, Z., Miller, W., and Lipman, D.J. (1997). Gapped BLAST and PSI-BLAST: a new generation of protein database search programs. Nucleic Acids Res. *25*, 3389–3402.
33. Mitchell, L.W., and Jaffe, E.K. (1993). Porphobilinogen synthase from *Escherichia coli* is a Zn(II) metalloenzyme stimulated by Mg(II). Arch. Biochem. Biophys. *300*, 169–177.